

Thermal expansion anisotropy of ternary molybdenum silicides based on Mo_5Si_3

J. H. Schneibel, C. J. Rawn, T. R. Watkins, and E. A. Payzant

Metals and Ceramics Division, Oak Ridge National Laboratory, Oak Ridge, Tennessee 37831

(Received 30 October 2001; revised manuscript received 17 January 2002; published 25 March 2002)

The coefficient of thermal expansion (CTE) of the tetragonal silicide Mo_5Si_3 is highly anisotropic. The ratio of the CTE's in the c and a directions, $\text{CTE}(c)/\text{CTE}(a)$, is approximately 2. Partial substitution of the Mo in Mo_5Si_3 by “larger” Nb or “smaller” V atoms increases or reduces the lattice parameters, respectively. In both cases the CTE anisotropy $\text{CTE}(c)/\text{CTE}(a)$ decreases significantly and values as small as 1.25 are observed. Similar results have been reported previously for Ti_5Si_3 alloyed with “large” Zr atoms and for Zr_5Si_3 alloyed with “small” Ti atoms. These results are interpreted in terms of the site occupation of the ternary alloying additions and the resulting reductions in the anharmonicity along the c axis.

DOI: 10.1103/PhysRevB.65.134112

PACS number(s): 65.20.+w, 61.10.Nz

I. INTRODUCTION

In noncubic crystal structures the coefficient of thermal expansion (CTE) can be highly anisotropic. Highly anisotropic thermal expansion in polycrystals results either in high degrees of strain¹ or in microcracking.² It is therefore of interest to understand and control the anisotropy of the thermal expansion.

Sometimes the CTE anisotropy changes significantly with alloying. This has been shown by Ikarashi *et al.*³ for the hexagonal isostructural compounds Ti_5Si_3 and Zr_5Si_3 . Their CTE anisotropies $\text{CTE}(c)/\text{CTE}(a)$ are 1.68 and 1.91, respectively. Surprisingly, the corresponding value for the isostructural ternary compound $\text{Ti}_2\text{Zr}_3\text{Si}_3$ was found to be 1.22 experimentally and 1.4 from first-principles calculations;⁴ i.e., the thermal expansion does not follow a rule of mixtures. In recent *ab initio* calculations of thermal expansion coefficients Fu and Wang⁵ suggested two principal factors for the high CTE anisotropy of Ti_5Si_3 . One is the relatively strong bonding in the (001) basal planes of its crystal structure. The other is related to the chains of closely spaced Ti atoms in the c direction (see Fig. 1 and Table I). According to Fu and Wang's calculations these atom chains along the c axis exhibit a high degree of anharmonicity and therefore the thermal expansion in the c direction is relatively high. It should also be noted that Fu and Wang suggested that alloying additions increasing the interatomic distance along the atom chains in the c direction might reduce the CTE anisotropy. The Goldschmidt radius of Zr is larger than that of Ti (1.57 vs 1.42 Å, respectively).⁶ Indeed, when Ti in Ti_5Si_3 is partially substituted by Zr to form the isostructural compound $\text{Ti}_2\text{Zr}_3\text{Si}_3$ the spacing along the Ti chains in the c direction increases and $\text{CTE}(c)$ decreases.³

In this paper we present experimental results showing the influence of ternary alloying additions on the CTE anisotropy of another highly anisotropic compound: namely, Mo_5Si_3 . Chu *et al.*⁷ recently measured the thermal expansion coefficients (CTE's) of Mo_5Si_3 single crystals and obtained $\text{CTE}(c)/\text{CTE}(a) = 2.21$, in substantial agreement with the theoretical value of 2 by Fu and Wang.⁵ Recent experimental work⁸ indicates that the CTE anisotropy ratio of Mo_5Si_3 can be reduced to values as low as 1.2 by partial substitution of Mo with “large” Nb atoms (the Goldschmidt

radii of Mo and Nb are 1.37 and 1.44 Å, respectively). This result is substantiated by the present work which was carried out with a parallel-beam x-ray diffractometer equipped with a precisely controlled (± 1 K) environmental chamber. It agrees qualitatively with first-principles calculations by Fu⁴ in which an anisotropy ratio of 1.5 was found for $(\text{Mo}_{0.2}\text{Nb}_{0.8})_5\text{Si}_3$. Following a suggestion by Fu,⁹ Mo_5Si_3 was also alloyed with V, which has a Goldschmidt radius smaller than that of Mo: namely, 1.33 Å. The results are interpreted in terms of Fu and Wang's *ab initio* calculations for Mo_5Si_3 . The CTE's of the $(\text{Ti,Zr})_5\text{Si}_3$ system are interpreted similarly and appear to follow the same physical mechanism.

II. EXPERIMENTAL DETAILS

Buttons of $(\text{Mo}_{1-x}\text{Nb}_x)_5\text{Si}_3$, $(\text{Mo}_{0.8}\text{V}_{0.2})_5\text{Si}_3$, and $(\text{Mo}_{0.4}\text{W}_{0.6})_5\text{Si}_3$ alloys with typical masses of 30 g were prepared from high-purity elements (typically 99.95%) by repeated arc melting in a partial pressure of argon followed by drop casting into 12.5-mm-diam Cu molds. The ingots were homogenized by annealing in vacuum for 24 h at 1600 °C followed by furnace cooling. Several ingots were sectioned and polished followed by examination in an optical microscope. Subsequently they were crushed into powders and screened to diameters ≤ 45 μm . High-temperature x-ray diffraction (HTXRD) data were collected using a Philips X'Pert PRO Θ - Θ diffractometer with an Anton-Paar XRK-900 high-temperature stage. The diffractometer was configured with an incident parabolic mirror and diffraction side 0.09°

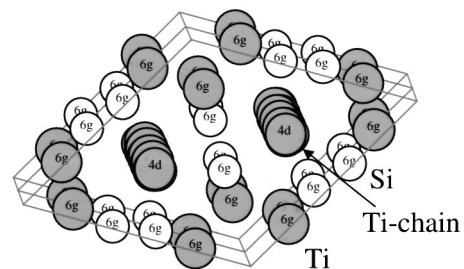


FIG. 1. Stack of two unit cells of the Ti_5Si_3 crystal structure viewed near the c direction.

TABLE I. Crystallographic data for Ti_5Si_3 and Mo_5Si_3 .

Compound	Structure type, Strukturbericht symbol,		Atom				Atomic spacing along chains in the c direction (Å)	Lattice parameters (Å)
	space group	Atom	Site ^a	x	y	z		
Ti_5Si_3	Mn_5Si_3	Ti	$4d$	1/3	2/3	0	2.572	
	$D8_8$	Ti	$6g$	0.2358	0	0.25		$a = 7.447$
	$P6_3/mcm$	Si	$6g$	0.5992	0	0.25		$c = 5.144$
Mo_5Si_3		Mo	$4b$	0	1/2	1/4	2.4545	
	W_5Si_3	Mo	$16k$	0.075	0.224	0		$a = 9.643$
	$D8_m$	Si	$4a$	0	0	1/4		$c = 4.909$
	$I4/mcm$	Si	$8h$	0.165	0.665	0		

^aWyckoff notation indicating how often a particular site (e.g., site b) occurs in the unit cell.

radial divergence limiting slits to achieve parallel beam optics. This configuration effectively removes any diffraction peak shifts resulting from the inherent displacement of the specimen surface due to thermal expansion. Data were collected in a continuous-scan mode using $\text{Cu } K_\alpha$ radiation with a step size of $0.02^\circ 2\theta$ and a count time of 1 s/step between $2\theta = [20^\circ, 70^\circ]$. The experiments were carried out in flowing He gas at 30 and 100 °C and then up to 600 °C in 100 °C intervals. The specimens were spun continuously to improve the particle statistics. Lattice parameters were evaluated using the Rietveld refinement module of the Philips X-Pert Plus software. For calibration purposes, the lattice parameters of an Al_2O_3 standard (NIST SRM 676, PDF 46-1212) were examined at room and elevated temperatures. The lat-

tice parameters indicated an accuracy $\Delta a/a$ and $\Delta c/c$ of approximately 1 part in 10 000 and an estimated precision of typically 5 parts in 100 000. The coefficients of thermal expansion were calculated from slopes of linear regression fits to plots of the lattice parameter versus temperature. The fits were constrained to the value of the lattice parameter at 30 °C and the slopes were divided by that value. The errors for the CTE ratios were obtained by propagating the errors of the standard errors for the individual CTE's.

III. EXPERIMENTAL RESULTS

Table II lists the nominal compositions of the alloys investigated and their lattice parameters at 30 °C. For refer-

TABLE II. Lattice parameters of ternary $(\text{Mo}_{1-x}\text{X}_x)_5\text{Si}_3$ at 30 °C. In addition to our experimental results, data obtained from the powder diffraction files (PDF) and from Chu *et al.* (Ref. 7) are listed. Also listed are the estimated standard deviations (esd) of the lattice parameters and the normalized changes in the lattice parameters due to alloying.

Ternary alloying element X	Ternary alloying element (at. %)	x in $(\text{Mo}_{1-x}\text{X}_x)_5\text{Si}_3$	a (Å)	esd (Å)	$a/a(\text{Mo}_5\text{Si}_3)$	c (Å)	esd (Å)	$c/c(\text{Mo}_5\text{Si}_3)$	Comments
n/a	0.0		9.65			4.911			Mo_5Si_3 , PDF 76-1578
n/a	0.0		9.59			4.87			Mo_5Si_3^a
n/a	0	0	9.6429	0.0004	1.000	4.9082	0.0003	1.000	Binary Mo_5Si_3
Nb	5	0.08	9.6696	0.0005	1.003	4.9251	0.0003	1.003	
Nb	12.5	0.2	9.7067	0.0004	1.007	4.9507	0.0003	1.009	
Nb	15	0.24	9.7220	0.0004	1.008	4.9587	0.0002	1.010	
Nb	30	0.48	9.8143	0.0005	1.018	4.9996	0.0003	1.019	
Nb	37.5	0.6	9.8660	0.0006	1.023	5.0194	0.0004	1.023	
Nb	37.5	0.6	9.8625	0.0005	1.023	5.0179	0.0003	1.022	
Nb	44	0.704	9.9071	0.0006	1.027	5.0323	0.0003	1.025	
Nb	44	0.704	9.9055	0.0006	1.027	5.0310	0.0003	1.025	
Nb	50	0.8	9.9467	0.0006	1.032	5.0442	0.0003	1.028	
Nb	56	0.896	9.9840	0.0004	1.035	5.0579	0.0002	1.030	
Nb	62.5	1	6.5685	0.0002	0.681	11.8815	0.0004	2.421	Binary Nb_5Si_3
Nb	62.5	1	6.5698			11.887			Nb_5Si_3 , PDF 30-0874
V	12.5	0.2	9.6048	0.0005	0.996	4.8643	0.0003	0.991	
W	37.5	0.6	9.6200	0.0001	0.998	4.9469	0.0001	1.008	

^aReference 7.

TABLE III. Coefficients of thermal expansion (CTE) including estimated error and regression coefficients R for Al_2O_3 .

CTE(a) (ppm/K)	Error (ppm/K)	R	CTE(c) (ppm/K)	Error (ppm/K)	R	CTE(c)/ TE(a)	Error	Reference
7.47	± 0.37		8.02	± 0.40		1.07	± 0.076	Al_2O_3 Ref. 10
7.14	± 0.14	0.9969	7.95	± 0.15	0.997	1.11	± 0.03	Al_2O_3 SRM676

ence, published data for Mo_5Si_3 and Nb_5Si_3 are listed as well. Our data for Mo_5Si_3 agree better with the powder diffraction file (PDF) data than the more recent results obtained by Chu *et al.*⁷ It should be noted that above $x \approx 0.9$ the crystal structure of $(\text{Mo}_{1-x}\text{Nb}_x)_5\text{Si}_3$ changes to the Cr_5B_3 structure type.

Table III compares results published for alumina¹⁰ with powder diffraction measurements carried out with the Philips X'Pert system for the alumina standard reference material. The good agreement with Touloukian's values¹⁰ shows that our system provides reliable results. Figure 2 shows the CTE's for $(\text{Mo}_{1-x}\text{Nb}_x)_5\text{Si}_3$ as a function of the Nb concentration x (see also Table IV). Whereas CTE(a) remains approximately constant, CTE(c) tends to decrease as the Nb concentration increases. Figure 3 shows the remarkable change in the ratio of the CTE's in the a and c directions due to alloying with Nb. Mo_5Si_3 exhibited pronounced microcracking on metallographic cross sections, whereas $(\text{Mo}_{0.4}\text{Nb}_{0.6})_5\text{Si}_3$ showed a much lower density of microcracks. This effect is attributed to the reduction in the CTE anisotropy due to alloying with Nb. Table IV shows that partial substitution of Mo with V is also effective in reducing the value of CTE(c)/CTE(a): for a V concentration of 12.5 at % a value of 1.5 was measured.

IV. DISCUSSION

Figure 4 shows the crystal structure of Mo_5Si_3 (see also Table I). As Mo in Mo_5Si_3 is partially substituted by Nb, the lattice parameters of the tetragonal unit cell increase. For $x \leq 0.48$, the normalized lattice parameter in the c direction, $c(\text{Mo}_{1-x}\text{Nb}_x)_5\text{Si}_3/c(\text{Mo}_5\text{Si}_3)$, increases more than in the a

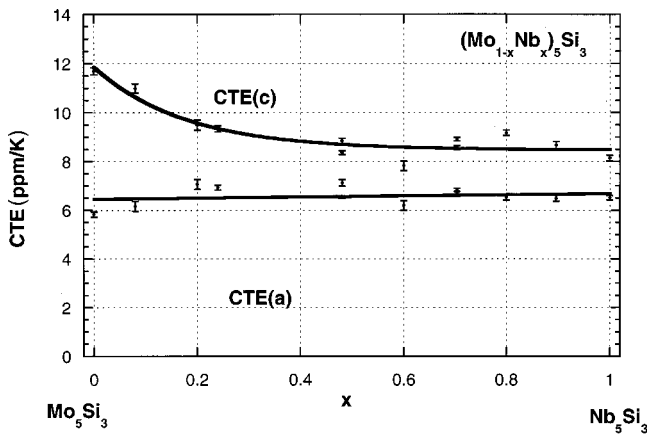


FIG. 2. Coefficients of thermal expansion for $(\text{Mo}_{1-x}\text{Nb}_x)_5\text{Si}_3$ in the a and c directions.

direction (see Table II). This is consistent with Fu and Wang's⁵ observation of exceptionally strong bonding in the basal plane. Since Nb is a larger atom than Mo, it likely prefers the relatively large $16k$ sites over the $4b$ chain sites. In doing so it increases the distance between the Mo atoms in the chains in the c direction. According to Fu and Wang, the stretching of the Mo chains in the c direction is associated with a reduction in the anharmonicity and the CTE in the c direction, as experimentally observed. Figure 2 shows that initially the CTE in the c direction decreases quickly: i.e., it is highly nonlinear with the Nb concentration. Above $x = 0.20$ the values of CTE(c)/CTE(a) in Fig. 3 are approximately constant, although there appears to be a small maximum near $x = 0.8$. In the absence of site occupation measurements (which would be difficult to perform since Mo and Nb have similar scattering cross sections for x rays and neutrons) and without a detailed theoretical model this part of the data cannot be interpreted at the present time.

When the Nb concentration is increased beyond $x \approx 0.9$ the crystal structure changes to the Cr_5B_3 structure type and the thermal expansion anisotropy is small. The thermal expansion of the compound Mo_5Si_2 , which has the same crystal structure as Cr_5B_3 , has been examined experimentally by Rawn *et al.*¹¹ and theoretically by Fu and Wang.⁵ Fu and Wang attribute its low thermal expansion anisotropy to the absence of a directionally bonded $[001]$ chain structure. We presume that this is the reason for the low CTE anisotropy of Nb_5Si_3 .

When Mo_5Si_3 is alloyed with 12.5 at. % V the c lattice parameter is proportionally reduced more than the a lattice parameter (0.89% vs 0.40%, respectively) and the CTE in the c direction decreases significantly. According to the above discussion for Nb additions, a decrease in the c lattice

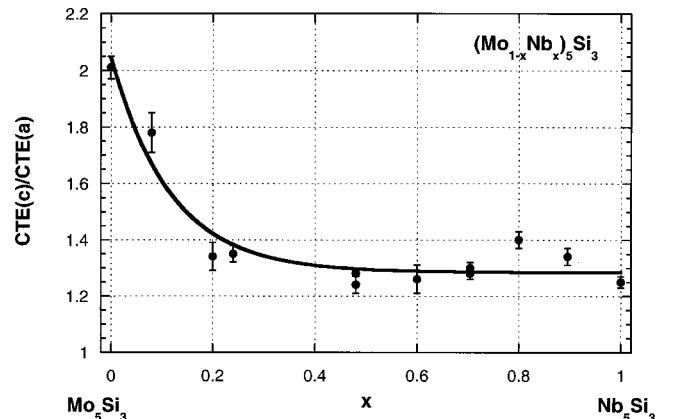


FIG. 3. Thermal expansion anisotropy of $(\text{Mo}_{1-x}\text{Nb}_x)_5\text{Si}_3$.

TABLE IV. Coefficients of thermal expansion (CTE) including estimated errors and regression coefficients R for binary and ternary compounds based on Mo_5Si_3 . The CTE data obtained by Chu *et al.* (Ref. 7) are also listed.

Ternary alloying element X	Ternary alloying element (at. %)	x in $(\text{Mo}_{1-x}\text{X}_x)_5\text{Si}_3$	CTE(a) (ppm/K)	Error (ppm/K)	R	CTE(c) (ppm/K)	Error (ppm/K)	R	CTE(c)/CTE(a)	Error	Comments
n/a	0.0	0.00	5.2			11.5			2.21		Mo_5Si_3^a
n/a	0	0	5.82	0.10	0.9973	11.69	0.15	0.9987	2.01	0.04	Binary Mo_5Si_3
Nb	5	0.08	6.16	0.20	0.9914	10.98	0.19	0.9976	1.78	0.07	
Nb	12.5	0.2	7.06	0.20	0.9934	9.49	0.21	0.9957	1.34	0.05	
Nb	15	0.24	6.93	0.10	0.9982	9.34	0.12	0.9985	1.35	0.03	
Nb	30	0.48	7.12	0.13	0.9971	8.84	0.11	0.9988	1.24	0.03	
Nb	30	0.48	6.51	0.04	0.9996	8.36	0.08	0.9992	1.28	0.01	
Nb	37.5	0.6	6.19	0.20	0.9908	7.82	0.20	0.9943	1.26	0.05	
Nb	44	0.704	6.68	0.09	0.9984	8.56	0.08	0.9992	1.28	0.02	
Nb	44	0.704	6.83	0.07	0.9990	8.91	0.07	0.9995	1.30	0.02	
Nb	50	0.8	6.53	0.13	0.9961	9.17	0.11	0.9988	1.40	0.03	
Nb	56	0.896	6.48	0.12	0.9972	8.67	0.15	0.9974	1.34	0.03	
Nb	62.5	1	6.51	0.09	0.9985	8.14	0.12	0.9981	1.25	0.02	Binary Nb_5Si_3
V	12.5	0.2	6.79	0.15	0.9960	10.23	0.16	0.9978	1.51	0.04	
W	37.5	0.6	4.89	0.06	0.9989	13.77	0.11	0.9992	2.82	0.04	

^aReference 7.

parameter would correspond to an increase in the anharmonicity and therefore an increase in the CTE in the c direction. Since this is not observed, the V must occupy the $4b$ Mo chain sites instead of the Mo $16k$ sites. This is consistent with the smaller atomic size of V as compared to Mo. In support of this argument, simulations of powder diffraction patterns using the software packages CRYSTMILLER and CRYSTALDIFFRACT (www.crystallmaker.com) were carried out. It was found that the low intensities of the experimentally observed (110) and (200) diffraction peaks were consistent with substitution of V on the $4b$ and not the $16k$ sites. We conclude that substitution of V on the Mo chain sites reduces the anharmonicity and the CTE in the c direction.

Alloying Mo_5Si_3 with V is qualitatively similar to alloying of hexagonal Zr_5Si_3 with Ti.³ When Zr_5Si_3 is alloyed with Ti both the a and c lattice parameters decrease. At the same time, the CTE in the c direction decreases. Again, this result suggests that the Ti substitutes for the Zr chain sites (the $4d$ sites in Fig. 1) instead of the larger $6g$ sites in the

structure and thus reduces the anharmonicity and thermal expansion in the c direction.

Substitutional alloying of Mo_5Si_3 does not necessarily reduce the CTE anisotropy. When Mo is partially substituted by W the CTE anisotropy actually increases: see Table IV. Again, this result is in qualitative support of our model: the model requires the ternary substitutional element to be either significantly larger or significantly smaller than the Mo atoms. Since the Goldschmidt radius of W is very similar to that of Mo (1.38 Å vs 1.37 Å), alloying with W is not expected to reduce the CTE anisotropy, as is experimentally observed. Similarly, partial substitution of Si in Ti_5Si_3 by Ge is not expected to change the thermal expansion anisotropy significantly. The reasons for this are that Ge and Si have similar atomic sizes and that there is only one type of site ($6g$) available for the Si or Ge atoms: see Fig. 1. Consistent with this argument the measurements of Williams *et al.*¹² show that, within experimental error, the CTE anisotropy ratios for Ti_5Si_3 and $\text{Ti}_5\text{Si}_{1.5}\text{Ge}_{1.5}$ are identical.

V. CONCLUSIONS

Alloying of Mo_5Si_3 with Nb, which is a larger atom than Mo, results in a pronounced decrease of the measured CTE anisotropy. The results are interpreted in terms of Fu and Wang's *ab initio* calculations for Mo_5Si_3 . It is suggested that the Nb substitutes initially for the relatively large Mo $16k$ sites instead of the small Mo $4b$ chain sites. By inserting Nb atoms on Mo sites other than the chain sites the Mo chains are stretched in the c direction. This reduces their anharmonicity and thereby the CTE in the c direction. Alloying with V also reduces the CTE in the c direction. In this case it is suggested that the relatively small V substitutes initially for the Mo chain sites, thus reducing the anharmonicity of the atomic interaction. Our results are qualitatively similar to

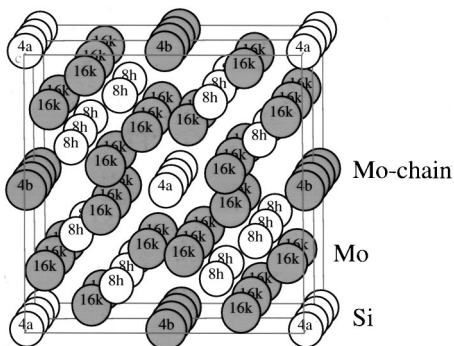


FIG. 4. Stack of two unit cells of the Mo_5Si_3 crystal structure viewed near the c direction.

earlier experimental results for the hexagonal $(\text{Ti,Zr})_5\text{Si}_3$ system and appear to follow the same physical model. It is suggested that these results apply generally to 5-3 compounds containing chain structures.

ACKNOWLEDGMENTS

This work was sponsored by the Division of Materials Sciences and Engineering, Office of Basic Energy Sciences,

and the Assistant Secretary for Energy Efficiency and Renewable Energy, Office of Transportation Technologies, as part of the High Temperature Materials Laboratory User Program, Oak Ridge National Laboratory. ORNL is operated by UT-Battelle, LLC, for the U.S. DOE under Contract No. DE-AC05-00OR22725. The considerable help of Chong Long Fu in discussing the experimental results is greatly appreciated. Thanks go also to W. D. Porter and R. K. Williams for their comments on the manuscript.

¹H. Shaked, J. D. Jorgensen, S. Short, O. Chmaissem, S.-I. Ikeda, and Y. Maeno, *Phys. Rev. B* **62**, 8725 (2000).

²A. J. Thom, M. K. Meyer, Y. Kim, and M. Akinc, in *Processing and Fabrication of Advanced Materials III*, edited by V. A. Ravi, T. S. Srivatsan, and J. J. Moore (TMS, Warrendale, PA, 1994), pp. 413–438.

³Y. Ikarashi, K. Ishizaki, T. Nagai, Y. Hashizuka, and Y. Kondo, *Intermetallics* **4**, S141 (1996).

⁴C. L. Fu (unpublished).

⁵C. L. Fu and X. Wang, *Philos. Mag. Lett.* **80**, 683 (2000).

⁶F. Laves, *Theory of Alloy Phases* (American Society for Metals, Cleveland, OH, 1956), pp. 124–198.

⁷F. Chu, D. J. Thoma, K. McClellan, P. Peralta, and Y. He, *Inter-*

metallics **7**, 611 (1999).

⁸J. H. Schneibel, C. J. Rawn, and C. L. Fu, in *High-Temperature Ordered Intermetallic Alloys IX*, edited by J. H. Schneibel, K. J. Hemker, R. D. Noebe, S. Hanada, and G. Sauthoff, MRS Symposia Proceedings No. 646 (Materials Research Society, Warrendale, PA, 2001), pp. N5.40.1–N5.40.6.

⁹C. L. Fu (private communication).

¹⁰*Thermophysical Properties of High Temperature Solid Materials*, edited by Y. S. Touloukian (Macmillan, New York, 1977).

¹¹C. J. Rawn, J. H. Schneibel, C. M. Hoffmann, and C. R. Hubbard, *Intermetallics* **9**, 209 (2001).

¹²J. J. Williams, M. J. Kramer, and M. Akinc, *J. Mater. Res.* **15**, 1780 (2000).